ELSEVIER

Cement & Concrete Composites 26 (2004) 665–675

Cement & Concrete Composites

www.elsevier.com/locate/cemconcomp

Optimisation of steel fibre reinforced concretes by means of statistical response surface method

F. Bayramov, C. Taşdemir *, M.A. Taşdemir

Department of Civil Engineering, Istanbul Technical University, Maslak, 80626 Istanbul, Turkey

Received 29 October 2002; accepted 25 June 2003

Abstract

The objective of this research is to optimise the fracture parameters of steel fibre reinforced concretes to obtain a more ductile behaviour than that of plain concrete. The effects of the aspect ratio (L/d) and volume fraction of steel fibre (V_f) on fracture properties of concrete in bending were investigated by measuring the fracture energy (G_F) and characteristic length (l_{ch}). For optimisation, three-level full factorial experimental design and response surface method were used. The results show that the effects of fibre volume fraction and aspect ratio on fracture energy and characteristic length are very significant.

Keywords: Fibre reinforced concrete; Steel fibre; Fracture energy; Characteristic length; Response surface method; Mix optimisation

1. Introduction

In this study, steel fibre reinforced concretes (SFRCs) are used as cement-based composite materials. These materials are reinforced with steel fibres. The fibres used are short, and their aspect ratio (length/diameter), volume fraction, and distribution as well as their matrix properties mainly influence the performance of SFRC. As a result of the rapid developments in concrete technology, concretes of strength over 100 MPa can be easily produced using ordinary materials and applying conventional mix design methods [1]. The main concern about high strength concrete is its increasing brittleness while its strength is being increased. The higher the strength of concrete, the lower is its ductility. This inverse relation between strength and ductility is a serious drawback when using high strength concrete is of concern. A compromise between these two conflicting properties of concrete can be obtained by adding short fibres [2]. Therefore, it becomes a more significant problem to improve the ductility of concrete. Steel fibre reinforcement greatly increases the energy absorption and ductility of concrete. For a better understanding of the fracture behaviour of concrete structures, knowledge of the post-cracking behaviour of concrete material is essential. The main contribution of steel fibres to concrete can mainly be observed after matrix cracking. If a proper design is made, after the matrix cracking, randomly distributed, short fibres in the matrix arrest microcracks, bridge these cracks, undergo a pull-out process and limit crack propagation [3,4]. Debonding and pulling out the fibres require more energy, therefore, a substantial increase in toughness, and resistance to cyclic and dynamic loading occurs [5]. ASTM C 1018 proposes a method for evaluating the toughness indices and JSCE-SF4 recommends determining the flexural toughness factor [6,7]. These two toughness parameters are not sufficient to define the tensile strain-softening law [8], which simulates the behaviour of the damaged region ahead of a continuous crack, which is referred to as the fracture process zone [5]. To define the softening behaviour, Hillerborg et al. [9] introduced the concept of fracture energy G_F. The standard test for the evaluation of this property was established by RILEM 50-FMC Technical Committee [10].

Until recently, the optimisation of SFRCs has been generally made by maximising the fracture energy (G_F). Li et al. [11] solved what was essentially an optimisation problem and also obtained approximate optimal values of fibre aspect ratio (L/d) and of the frictional bond

* Corresponding author. Tel.: +90-212-285-3771; fax: +90-212-285-6587.

E-mail address: tasdemir@itu.edu.tr (C. Taşdemir).

0958-9465/$ - see front matter © 2003 Elsevier Ltd. All rights reserved.
doi:10.1016/S0958-9465(03)00161-6

strength between the fibre-matrix by first relating the objective function G_F to these fibre parameters. In another work, Brandt [12] addressed to the issues about the simultaneous maximisation of G_F, compressive strength (f'_c), and the first cracking strength of FRC. These objective functions were related empirically to the mix, and the fibre variables. Lange-Kornbak and Karihaloo were the first to use mathematical optimisation techniques for the maximisation of G_F and f'_c (either separately or simultaneously) of SFRC [13,14]. They developed rigorous micromechanical relations between tensile strength and fracture energy, and the mix and fibre parameters.

In this study, a multiobjective simultaneous optimisation technique is used to optimise SFRC with special emphasis on ductility, in which response surface method (RSM) is incorporated. RSM, has been widely used to optimise products and processes in manufacturing, chemical and other industries, but it has had limited use in the concrete industry. In one study, Simon et al. [15] optimised High Performance Concrete mixtures using this method. The use of RSM to optimise SFRC mix design variables can significantly increase not only ductility (l_{ch}), but also splitting tensile strength (f_{st}). These two responses are of a conflicting nature, as can be seen from the following expression proposed by Hillerborg et al. [9]:

$$l_{ch} = \frac{G_F E}{f'^2_t} \tag{1}$$

where f'_t, E, and G_F are direct tensile strength, modulus of elasticity, and fracture energy, respectively.

1.1. Research significance

For improving the mechanical behaviour and fracture properties of SFRC with respect to aspect ratio and volume fraction of steel fibre, optimum design is needed. The effects of aspect ratio and volume fraction of steel fibre on the fracture energy and ductility were determined. Using the experimental results, splitting tensile strength, characteristic length and flexural strength were maximised simultaneously at the minimum steel fibre volume fraction. Thus, optimal values for the design parameters (L/d and V_f) were found while the brittleness of concrete is minimised.

2. Response surface modelling

Analysis of response surface over the simplex region involves the collection of experimental data, choosing a proper model that fits that data, and testing the adequacy of the fitted model. A response surface is the graph of system response as a function of one or more variables. These graphs offer an opportunity to visually analyse how certain factors influence the measurement system. To optimise a process or to find the best-fitting function of a number of experimental points, a model has to be found first; after this, the optimisation procedure is performed using the response surface of the model as the basis for finding the best solution. Without a model, optimisation does not lead to a general solution of the problem. In order to build a model, it is necessary to have some experimental data.

The main aim of this research is to provide the optimisation by maximising the characteristic length (l_{ch}), splitting tensile strength (f_{st}) and flexural strength at the minimum steel fibre volume fraction. For this purpose, a statistical RSM has been used. RSMs are tools for the modelling and analysis of problems where one or more measured responses are influenced by several factors and the objective is to optimise the response, such as the characteristic length (l_{ch}). RSM combines statistical and mathematical methods of experiment design, regression analysis and optimisation to provide useful approaches to the problem development, improvement, or optimisation. It provides a comprehensive, statistically based procedure for planning, executing, and evaluating batch [15].

A response surface can simultaneously represent two or more independent and one dependent variable when the mathematical relationship between the variables is known, or can be assumed. In this study, the dependent variables, or responses are compressive strength (f'_c), splitting tensile strength (f_{st}), flexural strength (f_{flex}), modulus of elasticity (E), fracture energy (G_F), and characteristic length (l_{ch}). Two factors (or independent x_k design variables) that can be selected to describe this system are fibre aspect ratio ($x_1 = L/d$), and fibre volume fraction ($x_2 = V_f$). Reasonable ranges can be given as follows:

$$\begin{aligned} &55 \leqslant L/d \leqslant 80 \\ &0.26\% \leqslant V_f \leqslant 0.64\% \end{aligned} \tag{2}$$

The additional limitations on the fibre properties given in the set of Eq. (2) are as follows:

For $55 \leqslant L/d \leqslant 65$, $L = 3(L/d) - 135$ and the ranges of L and d are $30 \leqslant L \leqslant 60$ mm and $0.55 \leqslant d \leqslant 0.92$ mm, respectively. For $65 \leqslant L/d \leqslant 80$, $L = 60$ mm and $0.75 \leqslant d \leqslant 0.92$ mm are specified, respectively.

A common response surface experimental plan which can be used to find optimal settings is a three-level, two variable full factorial experimental design. The full factorial design for $k = 2$ independent variables consists of $3^2 = 9$ points, that is $2^k = 2^2 = 4$ factorial points, $2k = 2 \times 2 = 4$ axial points and 1 centre point as plotted in Fig. 1.

For the use of a three-level, the two variable full factorial experimental design allows estimation of a full quadratic model for each response (i.e. f'_c, f_{st}, f_{flex}, E, G_F,

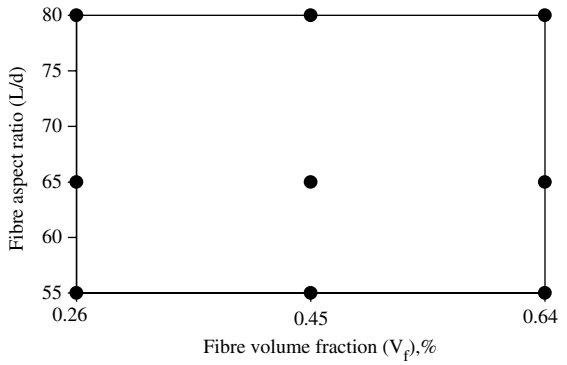

Fig. 1. Experimental design points according to three-level full factorial design.

and l_{ch}). The full quadratic model for two independent variables, which has 6 coefficients that are b_0, b_1, b_2, b_3, b_4, and b_5, is shown below:

$$y = b_0 + b_1x_1 + b_2x_2 + b_3x_1^2 + b_4x_2^2 + b_5x_1x_2 \quad (3)$$

The quadratic terms in (Eq. (3)) account for curvature in the response surface, which is often present when a response is at a maximum or minimum in the selected region [15].

3. Experimental details

3.1. Materials and mix proportions

A total of 10 concrete mixes were cast for this investigation. In all the mixes, the volume fractions of cement, siliceous sand, limestone fines, crushed limestone, and water were kept constant. Water to cement ratio was 0.36. Cement used was ordinary Portland cement with a density of 3.16 g/cm^3 and the cement content of concrete was 400 kg/m^3. Siliceous sand (0–0.25 mm) and limestone fines (0–4 mm) were used as fine aggregates; their densities were 2.63 and 2.65 g/cm^3, respectively. As coarse aggregate, crushed limestone was used. The maximum particle size of aggregate was 16 mm. The density of coarse aggregate was 2.65 g/cm^3. The amount of high-range water reducing admixture varied between 0.75% and 1.5% by weight of cement for different concrete mixtures to maintain sufficient workability. The volume fractions of steel fibres were 0.26%, 0.45%, and 0.64%, and the aspect ratios of fibres (L/d) were 55, 65, and 80. The properties of the steel fibres were given in Table 1. The concrete mixes were designated with the following codes: A and first two digits show the fibre aspect ratio, and V and the last two digits show the fibre volume fraction. For example, A80V64 indicates a mix with a fibre aspect ratio of 80 and a fibre volume fraction of 0.64%. NC denotes the control mix. Details of the mixtures are given in Table 2. This table also shows some properties of fresh concretes.

3.2. Specimen preparation

In mixing, cement, siliceous sand, limestone fines and crushed limestone were blended first and then, high-range water reducing admixture and water were added to the mix. Steel fibres were scattered on the mixture and carefully mixed to achieve a uniform distribution of the fibres in the concrete. Orientation of the fibres is generally random.

The specimens were cast in steel moulds and compacted on a vibration table. All the specimens were demoulded after about 24 h, stored in water saturated with lime, at 20 °C until 28 days old. At least three specimens of each concrete mix were tested under each type of loading condition at the 28th day. The beams prepared for the fracture energy tests were 500 mm in length and 100×100 mm in cross-section. Three cylinders were used for compressive tests; and for the splitting test, six disc specimens were prepared. Details of the tests and dimensions of the specimens are given in Table 3.

3.3. Test procedure

Standard strength tests were conducted in accordance with European Standards (EN 206 and EN 12390). For all the beams, the tests for the determination of the fracture energy (G_F) were performed according to the recommendation of RILEM 50-FMC Technical Committee [10]. Since the ratio of compressive strength to tensile strength of the SFRC tested in this work is in the range of 5 to 10, the method suggested by Hillerborg [16] and also pointed out by Barros and Figueiras [5] has been used. The effective cross-section, however, was reduced to 60×100 mm by sawing in order to accommodate both large aggregates and steel fibres used. The notched beam specimen tested is shown in the inset of Fig. 2. SFRC beam specimens were tested at the loading rate of 0.3 mm/min up to a deflection of 2 mm, and then at 1.5 mm/min up to a 5 mm deflection. As schematically

Table 1
The properties of the hooked-end steel fibres

Length (L), mm	Diameter (d), mm	Aspect ratio (L/d)	Density, g/cm^3	Tensile strength, N/mm^2
60	0.75	80	7.85	1050
60	0.92	65	7.85	1000
30	0.55	55	7.85	1100

Table 2
The details of mix concrete proportions

Mix code	NC	A55V26	A55V45	A55V64	A65V26	A65V45	A65V64	A80V26	A80V45	A80V64
Cement (C), kg/m^3	396	396	398	396	398	398	396	398	395	397
Siliceous sand, kg/m^3	281	281	283	281	282	283	281	282	280	281
Limestone fines (0–4 mm), kg/m^3	627	626	630	627	629	630	627	629	625	627
Crushed limestone (4–16 mm), kg/m^3	948	947	953	949	953	953	949	952	946	950
Water (W), kg/m^3	143	143	144	143	144	144	143	144	143	143
High-range water reducing admixture, % (kg/m^3)	0.75 (3)	0.8 (3.2)	0.85 (2.4)	1.0 (4)	1.09 (4.2)	1.04 (4.2)	0.97 (3.9)	1.23 (4.9)	1.33 (5.3)	1.45 (5.8)
W/C	0.36	0.36	0.36	0.36	0.36	0.36	0.36	0.36	0.36	0.36
Fibre volume fraction (V_f), %	–	0.26	0.45	0.64	0.26	0.45	0.64	0.26	0.45	0.64
Fibre aspect ratio (L/d)	–	55	55	55	65	65	65	80	80	80
Slump, cm	7	5	9	8	7	5.5	6	8	5	6.5
Unit weight, kg/m^3	2398	2415	2446	2450	2430	2447	2450	2430	2430	2454
Air content, %	1.57	1.41	0.65	0.78	0.74	0.47	0.79	0.71	1.08	0.51

seen in Fig. 2, the deflections were measured simultaneously by using two linear variable displacement transducers (LVDTs). The load was applied by an MTS of 250 kN maximum capacity. The load versus displacement curve for each specimen was obtained by recording the average of two measurements taken at the mid span.

4. Experimental results

The tests were carried out to investigate the effectiveness of steel fibre in the improvement of fracture energy and ductility with regard to the aspect ratio and fibre volume fraction.

4.1. Compressive strength

Compressive strength test results obtained from cylinder specimens are given in Table 4. The effect of the volume fraction of steel fibre seems to be more significant in concretes with the aspect ratio of 65. An increase of the fibre volume fraction (V_f) from 0.26% to 0.64% has resulted in an increase of 30% in the compressive strength. However, for the aspect ratio of 55 and 80, no significant change occurs when the fibre volume fraction is increased; thus the effect of the volume fraction of steel fibre on compressive strength is not consistent. However, the diameter of the steel fibre and possibly the orientation may have played an important role in compression. On the other hand, the addition of steel fibres into concrete may have an effect of increasing the ductility in the compressive failure rather than the compressive strength.

There is no significant effect of fibre volume fraction on the modulus of elasticity.

4.2. Splitting tensile strength

Splitting tensile strength of a disc specimen is calculated using the following expression:

$$f_{st} = \frac{2P}{\pi hd} \tag{4}$$

where P, h, and d are the ultimate load, height and diameter of the disc specimen, respectively.

Tensile strength values evaluated from splitting tests on disc specimens are included in Table 4 and plotted in Fig. 3. It is seen that the splitting tensile strength increases with increasing steel fibre volume fraction. As seen in Fig. 3 and Table 4, for the fibre aspect ratio of 55, an increase of the fibre volume fraction from 0 (i.e. normal concrete) to 0.64% has resulted in an increase of 23% in corresponding splitting tensile strength. For the aspect ratios of 65 and 80, this increase was 42% and 24%, respectively. Thus, it can be concluded that more

Table 3
Test methods and specimen size

Test type	Specimen	Dimensions (mm)	Parameters
Compression	Cylinder	∅150, $h = 300$	Compressive strength (f'_c), MPa Modulus of elasticity (E), GPa
Splitting	Disc	∅150, $h = 60$	Splitting tensile strength (f_{st}), MPa
Three-point bending	Beam	$100 \times 100 \times 500$	Fracture energy (G_F), N/m Flexural strength (f_{flex}), MPa

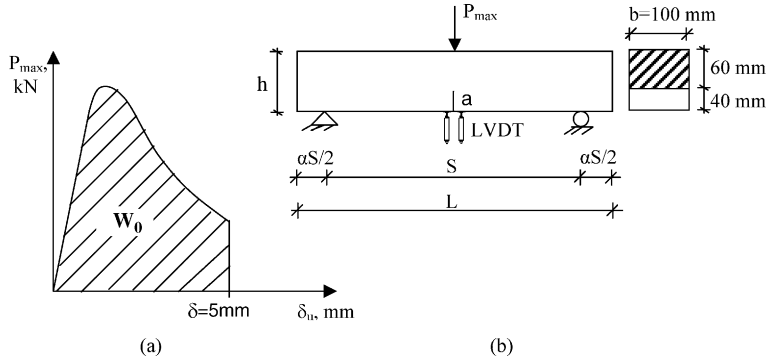

Fig. 2. Schematic representation of the evaluation of fracture energy (a), and test setup (b).

Table 4
Strength and fracture properties of concrete tested

Mix code	NC	A55V26	A55V45	A55V64	A65V26	A65V45	A65V64	A80V26	A80V45	A80V64
Compressive strength (f'_c), MPa	60.5	46.1	48.4	45.4	57.3	69.3	74.4	51.4	54.3	55.4
Flexural strength (f_{flex}), MPa	6.1	6.04	7.0	8.1	6.7	6.9	9.5	6.4	7.3	12.1
Splitting tensile strength (f_{st}), MPa	5.3	5.6	5.71	6.52	6.36	6.83	7.55	5.92	5.95	6.58
Modulus of elasticity (E), GPa	52.2	49.7	46.7	44.6	51.7	49.5	49.1	45.4	46.4	48.1
Fracture energy (G_F), N/m	91	1011	1851	3368	957	1939	3724	1024	1793	4371
Characteristic length (l_{ch}), mm	169	1599	2650	3537	1224	2056	3207	1327	2352	4845

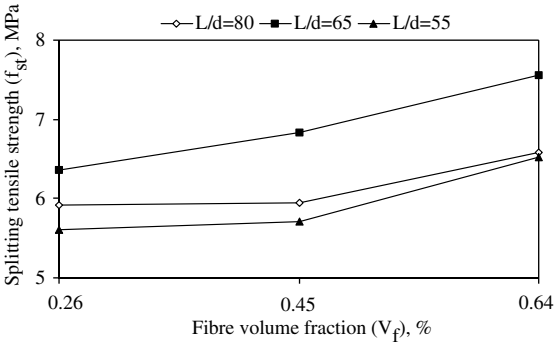

Fig. 3. Splitting tensile strength versus fibre volume fraction with different aspect ratio. (In NC, $f_{st} = 5.3$ MPa.)

significant results were obtained in SFRCs with the fibre aspect ratio of 65.

Along the fracture plane, the opening and propagation of the crack are controlled by the steel fibres. During the crack propagation some fibres are broken but some of them are pulled-out of the matrix. After completion of the splitting tests the fracture surfaces were examined. In most cases, the fibres with the aspect ratio of 65 ($L/d = 65$) did not break but were pulled out of the matrix. However, the fibres with the aspect ratio of 80 ($L/d = 80$) were broken into two parts. The results obtained for the fibres with $L/d = 65$ might be due to their larger cross-sections compared to that of fibres with $L/d = 80$. Similar results were obtained by Eren and Çelik [17]. The cylinder compressive strength of plain concrete used in this study is about 60 MPa, so for the steel fibres of $L/d = 80$, the mechanical mismatch between steel fibres and concrete may have also played a role in this behaviour. For high strength concrete, high strength steel fibre with a tensile strength of 2000 MPa is suggested [18,19].

4.3. Flexural strength

The flexural strength of a notched beam subjected to three-point bending test can be evaluated using the following equation:

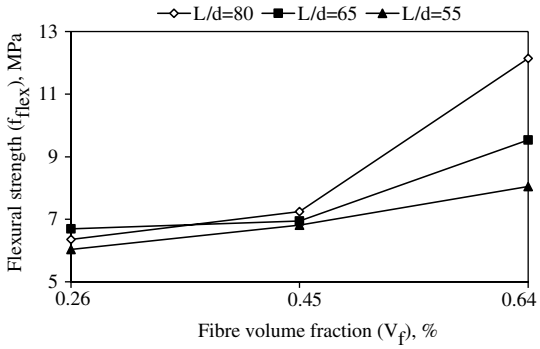

Fig. 4. Flexural strength versus fibre volume fraction with different aspect ratio. (In NC, $f_{flex} = 6.1$ MPa.)

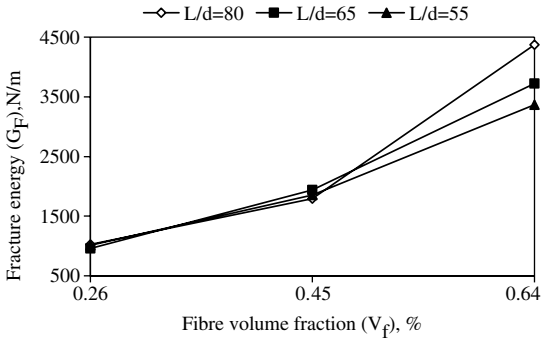

Fig. 5. Fracture energy versus fibre volume fraction with different aspect ratio. (In NC, $G_F = 91$ N/m.) Note that G_F for normal concrete was calculated from the mesomechanical relationships [21].

$$f_{flex} = \frac{3PS}{2b(h-a)^2} \tag{5}$$

where P is the ultimate load, and S, b, h, and a are span, thickness, height, and notch depth, respectively. Here, $a/h = 0.4$ and $S/h = 4$.

Flexural strengths of notched beams subjected to three-point bending tests are shown in Table 4. The effects of the aspect ratio and volume fraction of steel fibre on flexural strength are plotted in Fig. 4. The figure shows that, flexural strength increases as the fibre volume fraction increases. As seen in Fig. 4 and Table 4, for the fibre aspect ratio of 55, an increase in the fibre volume fraction from 0 (i.e. normal concrete) to 0.64%, has resulted in an increase of 33.5%. For the fibre aspect ratios of 65 and 80, the increases were 56.5% and 100%, respectively. The fracture process of steel fibre reinforced concrete consists of progressive debonding of fibre, during which slow crack propagation occurs. Final failure occurs due to unstable crack propagation when the fibres are pulled out and the interfacial shear stress reaches the ultimate strength. The reason for the increase in flexural strength is that, after matrix cracking, fibres carry the load subjected to concrete until the cracking of interfacial bond between fibres and matrix occurs. At higher aspect ratios, the advantage of using fibres for increasing flexural strength of concrete seems to be more significant [20].

4.4. Fracture energy

One of the major roles of fibre in concrete is to provide an increase in the energy required for fracture by the resultant crack arresting process. Fracture energy (G_F) is the energy needed to develop one crack completely. For a notched beam in three-point bending, the procedures recommended by RILEM TC 50-FMC Technical Committee were applied to measure G_F. The load–deflection curves were used for evaluating the fracture energy. The area under the load versus deflection at mid span curve (W_0) was described as a measure of the fracture energy of the material. The results obtained here are based on the area under the complete load–deflection curve up to a specified deflection. The cut-off point was chosen as 5 mm deflection. It is seen from the schematic curve that, the energy at this deflection (i.e. 5 mm), however is not totally dissipated. As shown in Fig. 2, this property was determined using the following expression [10]:

$$G_F = \frac{W_0}{b(h-a)} + \frac{m(1-\alpha^2)g\delta}{b(h-a)} = G_F^{(a)} + G_F^{(b)} \tag{6}$$

where b, h, a, m, and S are the width, depth, notch depth, weight of the beam between the supports, and span, respectively. g is the gravity acceleration, $\alpha = \frac{L}{S} - 1$, δ is the deflection of the beam (5 mm) and, $G_F^{(a)}$ and $G_F^{(b)}$ are the fracture energies supplied by actuator and the beam weight, respectively.

G_F of the mixes are shown in Fig. 5, and also in Fig. 9, expressed as a function of the aspect ratio and volume fraction of steel fibre. It can clearly be seen that fracture energy increases as the fibre volume fraction increases. As seen in Fig. 5 and Table 4, these SFRCs allow obtaining high values of fracture energies and as a result a high ductility; depending on their aspect ratios and volume fractions of fibres used. The ductility is more than about 40 times greater than that of normal concrete. The increase in the fracture energy is because of the high energy of fibre pull-out and fibre debonding in the fracture process. The reason for the increase in fracture energy with increasing fibre volume fraction and its aspect ratio stems from a great number of fibres forming a bridge in the crack forming tortuous crack propagation.

4.5. Characteristic length

Characteristic length (l_{ch}) should be taken into consideration in the design of concrete mixes, because it controls the nominal strength, failure mode, and crack growth (crack pattern) [13]. In order to obtain the

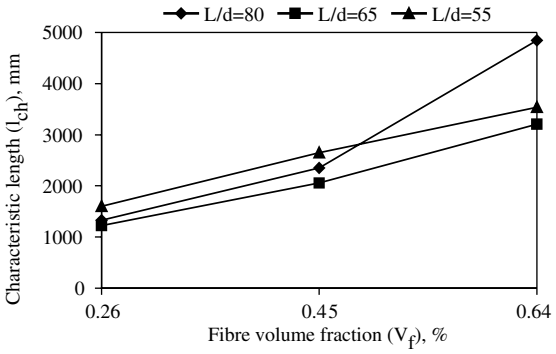

Fig. 6. Characteristic length versus fibre volume fraction with different aspect ratio. (In NC, $l_{ch} = 169$ mm.)

ductility of the mixes, l_{ch} was calculated using the measured G_F, E and f'_t according to (Eq. (1)) introduced in the fictitious crack model by Hillerborg et al. [9]. In this study the direct tensile strength (f'_t) term in this relation was replaced by splitting tensile strength (f_{st}). The variation of l_{ch} with L/d and V_f is shown in Fig. 6. As seen in Fig. 6 and Table 4, as both aspect ratio and volume fraction of the steel fibre increase, the characteristic length which is a measure of ductility of the mix, increases significantly. Hence, it can be concluded that the results obtained give a clear picture of how a quasi-brittle concrete transforms into a ductile composite with the addition of steel fibres.

5. Regression analysis

It is very important to choose an appropriate model for describing the shape of the surface for each response. Each mechanical response of SFRC is analysed individually by examining summary plots of the data, fitting a full quadratic model using ANOVA, validating the model by examining the residuals for trends and outliers, and interpreting the model graphically. A full quadratic model can be estimated with a three-level full factorial design, but some of the terms may not be significant. The full quadratic model was simplified by using a backward stepwise technique. The only way to accept or reject a certain explanation term is to test its significance in order to ensure that the additional term really contributes to the explanation of the response. The procedure to specify an appropriate model is presented below:

1. Fit the full quadratic model and for each coefficient, calculate the t-statistic for the null hypothesis that the coefficient is equal to zero.
2. Perform the regression again with a partial model containing only those terms that are statistically significant (i.e. those terms that had a t-statistic greater than that of the chosen significance level, in this study $\alpha = 0.05$). Calculate t-statistics again and eliminate any insignificant terms, and repeat this procedure until the partial model contains only significant terms.

Thus, nine experimental data were fitted to a polynomial type of mathematical model by adjusting parameters until calculated values were in close agreement with the experimental values. Model fitting results for each response are shown in Table 5.

For fracture energy (G_F), the fitted regression model was

$$G_F = 3542.1 - 33.64(L/d) - 11514V_f + 13468.16V_f^2 + 103.41(L/d)V_f \quad (7)$$

In this case (L/d), V_f, V_f^2, and $(L/d)V_f$ are the significant terms. In the analyses of each response, only significant terms ($\alpha < 0.05$) were included in the model. Using the same procedure described above for G_F, the following models (Eqs. (8)–(12)) were used for compressive strength (f'_c), splitting tensile strength (f_{st}), modulus of elasticity (E), flexural strength (f_{flex}) and characteristic length (l_{ch}):

$$f'_c = -530.12 + 17.26(L/d) + 17.75V_f - 0.13(L/d)^2 \quad (8)$$

$$f_{st} = -21.68 + 0.84(L/d) - 2.91V_f - 0.01(L/d)^2 + 5.98V_f^2 \quad (9)$$

$$E = -15.89 + 2.48(L/d) - 74.42V_f - 0.02(L/d)^2 + 17.15V_f^2 + 0.82(L/d)V_f \quad (10)$$

Table 5
Model fitting results for each response

Responses	Coefficients					
	b_0	b_1	b_2	b_3	b_4	b_5
f'_c	−530.12	17.26	17.75	−0.13	–	–
f_{st}	−21.68	0.84	−2.91	−0.01	5.98	–
E	−15.89	2.48	−74.42	−0.02	17.15	0.82
f_{flex}	16.67	−0.12	−44.64	–	30.22	0.40
G_F	3542.1	−33.64	−11514	–	13468.16	103.41
l_{ch}	21687.6	−600.43	−5080.32	3.95	–	173.53

Table 6
Fitted values for each mechanical properties of SFRC

Fibre aspect ratio (L/d)	Fibre volume fraction (V_f), %	Fitted values					
		Compressive strength (f'_c), MPa	Splitting tensile strength (f_{st}), Mpa	Flexural strength (f_{flex}), MPa	Modulus of elasticity (E), GPa	Fracture energy (G_F), N/m	Characteristic length (l_{ch}), mm
80	0.64	57.1	6.7	11.8	48.1	4251	4523
80	0.45	53.7	6.0	7.9	46.2	2084	2841
80	0.26	50.3	5.8	6.2	45.6	900	1159
65	0.64	71.7	7.5	9.7	49.1	3767	3286
65	0.45	68.3	6.8	6.9	49.6	1896	2101
65	0.26	64.9	6.6	6.4	51.3	1009	917
55	0.64	50.0	6.5	8.3	44.5	3445	3448
55	0.45	46.6	5.8	6.3	46.6	1772	2595
55	0.26	43.2	5.6	6.5	49.9	1082	1742

$$f_{flex} = 16.67 - 0.12(L/d) - 44.64V_f + 30.22V_f^2 + 0.4(L/d)V_f \quad (11)$$

$$l_{ch} = 21687.6 - 600.43(L/d) - 5080.32V_f + 3.95(L/d)^2 + 173.53(L/d)V_f \quad (12)$$

By using the Eqs. (7)–(12), the fitted values that were obtained for each of the mechanical properties of SFRC are shown in Table 6. Response surfaces of the mechanical properties, f_{st}, f_{flex}, G_F, and l_{ch} as a function of the aspect ratio and volume fraction of steel fibre are plotted in Figs. 7–10, respectively.

6. Optimisation

After building the regression model and establishing relationships between mix design variables and the responses expressed in Eqs. (7)–(12), all independent

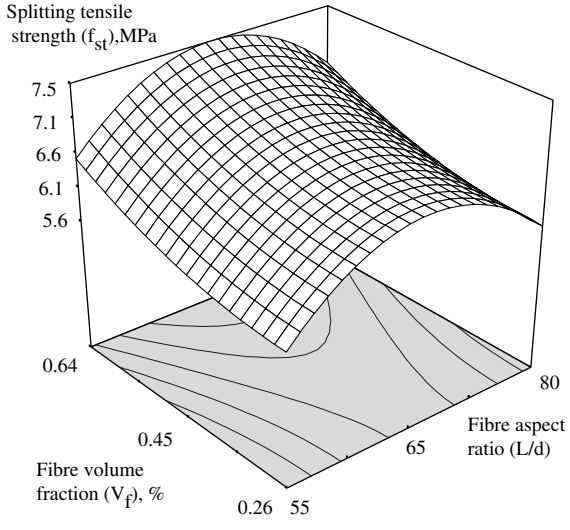

Fig. 7. The variation of f_{st} with L/d and V_f.

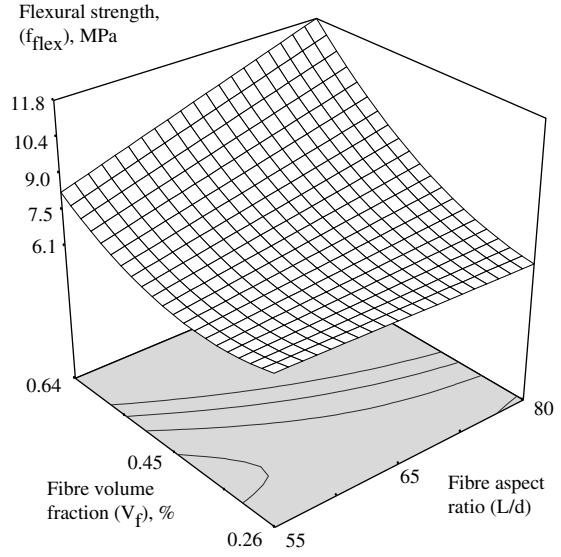

Fig. 8. The variation of f_{flex} with L/d and V_f.

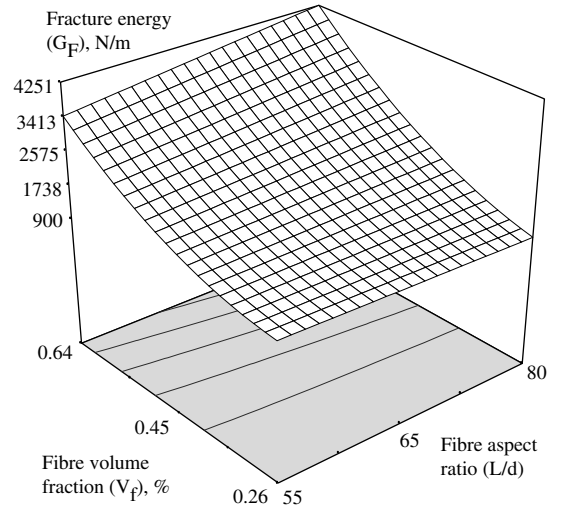

Fig. 9. The variation of G_F with L/d and V_f.

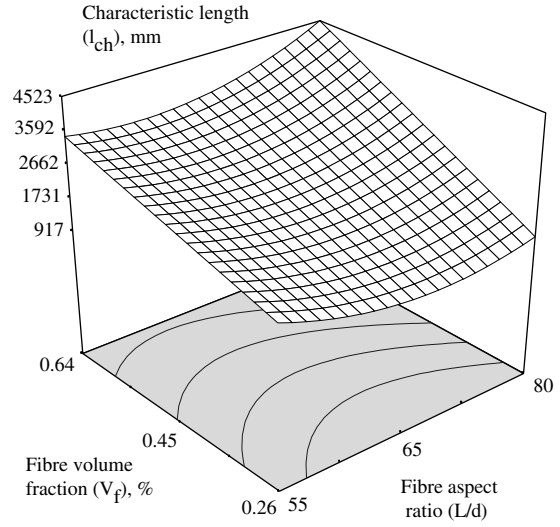

Fig. 10. The variation of l_{ch} with L/d and V_f.

variables are varied simultaneously and independently in order to optimise the objective functions. The objective of optimisation is to find the "best settings" that maximise a particular response or responses. Optimisation usually involves considering several responses simultaneously. A numerical optimisation technique using desirability functions (d_j), which are defined for each response, can be used to optimize the responses simultaneously [22]. A desirability function (d_j) varies over the range of $0 \leqslant d_j \leqslant 1$. By using the single composite response (D) given in Eq. (13), which is the geometric mean of the individual desirability functions, the multiobjective optimisation problem is solved. D is maximised over the feasible region of the design variables given in Eq. (2) [23]:

$$D = (d_1 \times d_2 \times d_3 \times \cdots \times d_n)^{\frac{1}{n}} \tag{13}$$

where n is the number of responses included in the optimisation. If any of the responses or factors falls outside their desirability range, the overall function becomes zero.

In cases of the maximising and minimising of individual responses, the desirability will be defined by the formulas given in Eqs. (14) and (15), respectively.

$$d_j = \begin{cases} 0 & Y_j \leqslant \min f_j \\ \left[\frac{Y_j - \min f_j}{\max f_j - \min f_j}\right]^{wt_j} & \text{and } 0 < d_j < 1, \\ & \min f_j < Y_j < \max f_j \\ 1 & Y_j \geqslant \max f_j \end{cases} \tag{14}$$

$$d_j = \begin{cases} 1 & Y_j \leqslant \min f_j \\ \left[\frac{\max f_j - Y_j}{\max f_j - \min f_j}\right]^{wt_j} & \text{and } 0 < d_j < 1, \\ & \min f_j < Y_j < \max f_j \\ 0 & Y_j \geqslant \max f_j \end{cases} \tag{15}$$

where d_j, Y_j, min f_j and max f_j are the desirability function, the fitted value, and minimum and maximum actual (experimental) values of jth response included in the optimisation, respectively. The power value wt_j is a weighting factor of the jth response.

In this work, for optimisation, a commercially available (Design-Expert) software package was used.

To attain a less brittle concrete, a concrete with the highest splitting tensile strength (f_{st}), the highest characteristic length (l_{ch}) and also the highest flexural strength (f_{flex}) is to be obtained. So it is necessary to maximise f_{st}, l_{ch} and f_{flex}, simultaneously. Thus, these three responses (f_{st}, l_{ch} and f_{flex}) are considered to be of equal importance, i.e. $wt_j = 1$ and maximised simultaneously. For $n = 3$, Eq. (13) takes on the form:

$$D = (d_1 \times d_2 \times d_3)^{\frac{1}{3}} \tag{16}$$

where d_1, d_2 and d_3 are the desirability functions of f_{st}, l_{ch} and f_{flex}, respectively.

The solution of this multiobjective optimisation is shown in Fig. 11. The figure shows that, the optimal values of design variables are $V_f = 0.64\%$ and $L/d = 76.44$. Since $65 \leqslant L/d \leqslant 80$, the limitations of L and d are: $L = 60$ mm and $0.75 \leqslant d \leqslant 0.92$ mm, thus $L = 60$ mm and $d = 0.785$ mm, which shows that d is between 0.75 and 0.92. The predicted response values and associated uncertainties (at 95% confidence level) are $l_{ch} = 4068 \pm 415$ mm, $f_{st} = 7.1 \pm 0.2$ MPa, $f_{flex} = 11.3 \pm 0.7$ MPa, $G_F = 4136 \pm 237$ N/m, $E = 49.2 \pm 0.4$ GPa and $f'_c = 65.7 \pm 4.7$ MPa.

The cost of the steel fibres used in the production of composites is also important from the application is of concern. Therefore, the volume fraction of steel fibre must be minimised to get an economical mixture. Numerical optimisation can optimise any combination of either factors or responses. Thus, f_{st}, l_{ch}, f_{flex} and volume fraction of steel fibre (V_f) are also considered to be of

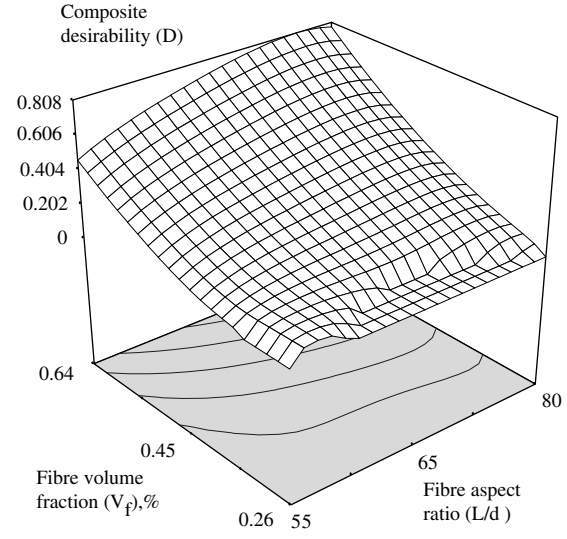

Fig. 11. Response surface plot of the composite desirability (D) when f_{st}, l_{ch} and f_{flex} are maximised simultaneously.

equal importance, i.e. $wt_j = 1$ and optimised simultaneously, i.e. f_{st}, l_{ch} and f_{flex} are maximised and V_f is minimised. In this case Eq. (13) takes on the form:

$$D = (d_1 \times d_2 \times d_3 \times d_4)^{\frac{1}{4}} \quad (17)$$

where d_1, d_2, d_3, and d_4 are the desirability functions of f_{st}, l_{ch}, f_{flex} and V_f, respectively.

The solution of this multiobjective optimisation is shown in Figs. 12 and 13. These figures show that, the optimal values of design variables are $V_f = 0.558\%$ and $L/d = 75.87$, i.e. $L = 60$ mm, $d = 0.791$ mm, and $V_f = 0.558\%$. The predicted response values and associated uncertainties (at 95% confidence level) are $l_{ch} = 3359 \pm 310$ mm, $f_{st} = 6.8 \pm 0.1$ MPa, $f_{flex} = 9.4 \pm 0.5$ MPa, $G_F = 3125 \pm 165$ N/m, $E = 48.6 \pm 0.3$ GPa and $f'_c = 65 \pm 3.8$ MPa.

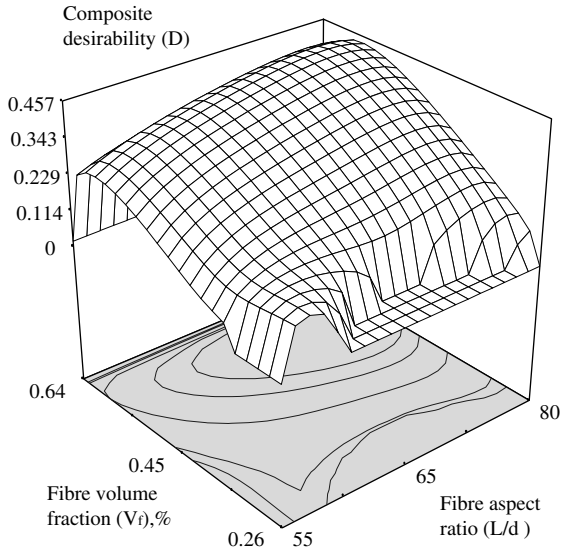

Fig. 12. Response surface plot of the composite desirability (D) when f_{st}, l_{ch} and f_{flex} are maximised and steel fibre volume fraction (V_f) is minimised simultaneously.

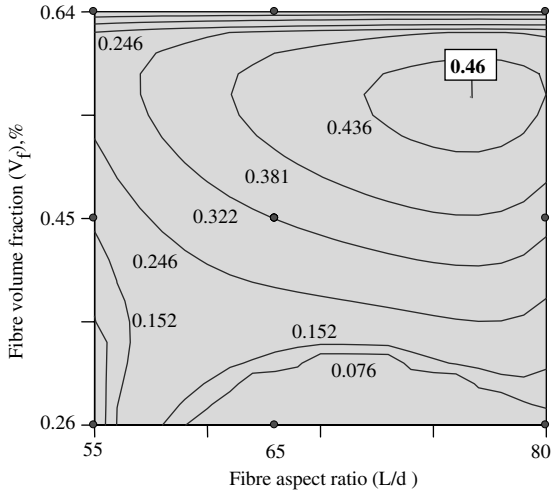

Fig. 13. Contour plot of the composite desirability (D) when f_{st}, l_{ch} and f_{flex} are maximised and steel fibre volume fraction (V_f) is minimised simultaneously.

7. Concluding remarks

Response surface method is a promising approach for optimising SFRCs to meet several performance criteria such as minimum brittleness. The experimental design made by using RSM provides a thorough examination of SFRC properties over the selected range of fibre volume fraction and aspect ratio. In order to provide an adequate representation of the responses, fitting quadratic models that are usually assumed to represent each concrete property of interest, can be done in identifying optimal mixes. The results show that the predictiveness of the polynomial regression model is satisfactory. The addition of steel fibre improves fracture properties significantly.

When the mechanical properties (f_{st}, l_{ch} and f_{flex}) are concerned, the optimal values of design variables obtained are as follows: a steel fibre volume fraction of 0.64% and an aspect ratio of 76.44. For both mechanical properties (f_{st}, l_{ch} and f_{flex}) and cost optimisation the optimal values of design variables obtained are as follows: a steel fibre volume fraction of 0.558% and an aspect ratio of 75.87.

Compatibility of the matrix with the steel fibre should be investigated and an optimisation based mixture design is to be used as a future work.

Acknowledgements

The financial support of TUBITAK (The Scientific and Technical Research Council of Turkey)—BAYG is greatly appreciated by the first author. The second and third authors wish to acknowledge the grant of The British Council (Britain–Turkey Partnership Program for the academic link between ITU and Cardiff University), and the financial supports of TUBITAK (Project: ICTAG 1665) and DPT (State Planning Organization, Project: 2002K120340). The support given by BEKSA is also gratefully acknowledged.

References

[1] Balaguru P, Narahari R, Patel M. Flexural toughness of steel fibre reinforced concrete. ACI Mater J 1992;89(6):541–6.
[2] Wafa FF, Ashour SA. Mechanical properties of high-strength fibre reinforced concrete. ACI Mater J 1992;89(5):449–55.
[3] Banthia N, Trottier JF. Concrete reinforced with deformed steel fibres. Part II: Toughness characterization. ACI Mater J 1995;92(2):146–54.

[4] Kurihara N, Kunieda M, Kamada T, Uchida Y, Rokugo K. Tension softening diagrams and evaluation of properties of steel fibre reinforced concrete. Eng Fract Mech 2000;65:235–45.
[5] Barros JAO, Figueiras JA. Flexural behaviour of SFRC: testing and modelling. J Mater Civ Eng 1999;11(4):331–9.
[6] ASTM. Standard test method for flexural toughness and first-crack strength of steel fibre reinforced concrete (using beam with third-point loading), ASTM C 1018-97, Philadelphia, 1997.
[7] JSCE-SF4. Method of tests for flexural strength and flexural toughness of steel fibre reinforced concrete. Concrete Library of JSCE. Japan Society of Civil Engineers (JSCE), Tokyo, vol. 3, 1984, p. 58–61.
[8] Hordijk DA. Local approach to fatigue of concrete. PhD dissertation. Delft University of Technology, Delft, Netherlands, 1991.
[9] Hillerborg A, Modeer M, Peterson PE. Analysis of crack formation and crack growths in concrete by means of fracture mechanics and finite elements. Cem Concr Res 1976;6:773–82.
[10] RILEM 50-FMC. Committee of fracture mechanics of concrete. Determination of fracture energy of mortar and concrete by means of three-point bend tests on notched beams. Mater. Struct. 1985;18(106):285–90.
[11] Li VC, Wang Y, Backer SA. Micromechanical model of tension softening and bridging toughening of short random fibre reinforced brittle matrix composites. J Mech Phys Solids 1991;39:607–25.
[12] Brandt AM. Cement-based composites, materials, mechanical properties and performance. London: E & FN Spon; 1995.
[13] Lange-Kornbak D, Karihaloo BL. Design of fibre-reinforced DSP mixes for minimum brittleness. Adv Cem Based Mater 1998;7:89–101.
[14] Karihaloo BL, Lange-Kornbak D. Optimisation technique for the design of high-performance fibre-reinforced concrete. Struct Multidiscip Optimisation 2001;21(1):32–9.
[15] Simon MJ, Lagergren ES, Wathne LG. Optimising high-performance concrete mixtures using statistical response surface methods. In: Proceedings of the 5th International Symposium on Utilization of High Strength/High Performance Concrete. Oslo, Norway: Norwegian Concrete Association; 1999. p. 1311–21.
[16] Hillerborg A. Concrete fracture energy tests performed by 9 laboratories according to a draft RILEM recommendation. Report to RILEM TC 50-FMC, Report TVBM-3015, Lund Institute of Technology, Lund, Sweden, 1983.
[17] Eren Ö, Çelik T. Effect of silica fume and steel fibers on some properties of high-strength concrete. Constr Build Mater 1997;11(7–8):373–82.
[18] Vandewalle L. Influence of the yield strength of steel fibres on the toughness of fibre reinforced high strength concrete. In: Proceedings, the CCMS Symposium, Worldwide Advances in Structural Concrete and Masonry. Chicago, 1996, p. 496–505.
[19] Grünewald S, Walraven JC. High strength self-compacting fibre reinforced concrete: behaviour in the fresh and hardened state. In: König G et al., editor. 6th International Symposium on HSC/HPC, vol. 2, Leipzig, June 2002, p. 977–89.
[20] Gao J, Sun W, Morino K. Mechanical properties of steel fibre-reinforced, high-strength, lightweight concrete. Cem Concr Compos 1997;19:307–13.
[21] Lange-Kornbak D, Karihaloo BL. Design of concrete mixes for minimum brittleness. Adv Cem Based Mater 1996;3:124–32.
[22] Derringer G, Suich R. Simultaneous optimization of several response variables. J Qual Technol 1980;12(4):214–9.
[23] Myers RH, Montgomery DC. Response surface methodology: process and product optimization using designed experiments. New York: John Wiley & Sons; 2002.